Forced convection heat transfer of Giesekus fluid with wall slip above the critical shear stress in pipes

Mehdi Moayed Mohseni, Gilles Tissot, Michael Badawi

Forced convection heat transfer of Giesekus fluid with wall slip above the critical shear stress in pipes

Mehdi Moayed Mohseni[a],*, Gilles Tissot[b], Michael Badawi[a],*

[a] Laboratoire Physique et Chimie Théoriques (LPCT, UMR CNRS UL 7019), Institut Jean Barriol, Université de Lorraine, Rue Victor Demange, 57500 Saint-Avold, France.
[b] Laboratoire d'Acoustique de l'Université du Mans - UMR CNRS 6613 Avenue Olivier Messiaen 72085 Le Mans cedex 09.

 * Corresponding authors: mehdi.moayed.mohseni@gmail.com; michael.badawi@univ-lorraine.fr

Highlights

- **Increasing slip effect increase Nusselt number in Br>0.**

- **Nusselt number decrease by increasing Brinkman number in Br>0.**

- **For the cooling case fluid starts to warm up in Br>Br_1.**

- **Nusselt curve show a singularity in Br_2.**

- **Br_1 and Br_2 increase by Increasing slip effect.**

Abstract

Forced convective heat transfer in pipes is investigated for viscoelastic fluids obeying the Giesekus constitutive equation including effect of slip condition by an approximated analytical method. The slip equation at wall is considered nonlinear Navier model with non-zero slip critical shear stress. The problem under consideration is steady, laminar and fully developed. Thermal boundary conditions are assumed peripherally and axially constant heat flux at wall. The fluid heating and cooling cases are considered for analysis. Dimensionless temperature profiles and Nusselt number are obtained by solving governing equations and the effects of slip parameters, viscous dissipation and fluid elasticity are

discussed. Results show that Nusselt number increases by increasing slip effect but decreases by increasing Brinkman number for the case of fluid heating. However, for the cooling case, the heat generated by viscous dissipation can overcome the effect of wall cooling at first critical Brinkman number and fluid starts to warm up. Also the Nusselt curve shows a singularity in a second critical Brinkman number.

1. Introduction

The heating and cooling processes have to use the non-Newtonian fluids in a broad variety of equipment and industries related to fluid such as shell and tube heat exchangers, polymer and plastic extrusion, drilling operations and food industries [1,2]. Therefore, the knowledge of heat transfer is mandatory for the equipment design and quality control of the final products. Also the empirical evidences indicate that, in certain circumstances, most of these complex fluids may be slipped at the solid boundary which again has a strong influence to quality of final products such as sharkskin, stick-slip, and gross melt fracture instabilities in polymer extrusion. Slip can be occurred by three mechanisms as below:

- Adhesive failure of the polymer chains on the solid surface leading to detachment of the absorbed chains from the wall.
- Cohesive failure arising from disentanglement of the bulk chains from chains adsorbed at the wall, and then disentangled chains will slip over adsorbed chains.
- Formation of a low viscosity layer of solvent which is known to low-viscosity mesophase and the bulk polymer chains slip on this layer.

One of the most common models for determine the slip velocity at the wall is the nonlinear Navier slip law which is based on experimental results and consists in a power law relationship between slip velocity and shear stress at the wall as follows:

$$u_w = \left(\frac{|\tau_w|}{\beta}\right)^{\frac{1}{s}}$$
(1)

where u_w, τ_w and s are the slip velocity, shear stress at wall and power law index respectively.

β is the slip coefficient which depends on temperature, normal stress, molecular parameters and properties of the fluid/wall interface [3]. As $\beta \to 0$ full slip flow and $\beta \to \infty$ no slip boundary condition are recovered. . Fig.1 shows the Hagen–Poiseuille velocity profile for slip and no slip boundary conditions.
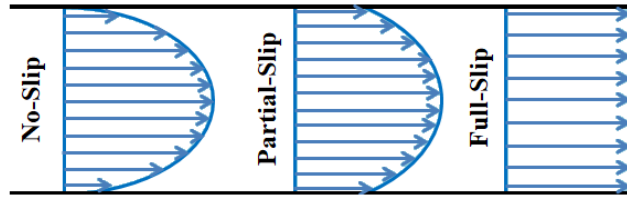

Fig. 1. Schematic diagram of Poiseuille flow with slip boundary conditions.

Since the empirical evidence shows the slip occurs only when wall shear stress exceeds a critical value [4] therefore the nonlinear Navier slip model is employed under the following form:

$$\begin{cases} u_w = 0 & |\tau_{rz\,w}| \le \tau_c \\[2mm] u_w = \left(\frac{|\tau_{rz\,w}| - \tau_c}{\beta}\right)^{\frac{1}{s}} & |\tau_{rz\,w}| > \tau_c \end{cases}$$
(2)

Effect of slip condition in the flow field of Newtonian and non-Newtonian fluids has been investigated extensively [5-16] but research on heat transfer is scant. Analytical solutions for heat transfer and entropy generation of Newtonian fluid in microchannel were obtained by Anand [17] considering slip boundary conditions. The non-linear Navier, Hatzikiriakos and asymptotic slip laws were employed and the microchannel walls were subject to uniform heat flux. Finally, the effect of slip at walls on velocity distribution, temperature distribution, Nusselt number, entropy generation rate and Bejan number has been reported in this paper. Shojaeian and Kosar [18] investigated effect of slip condition on convective heat transfer and entropy generation for Newtonian and non-Newtonian fluid using the linear Navier slip model between parallel-plates. The thermal boundary conditions were assumed isoflux and

isothermal and the expressions for velocity, local and mean temperature distributions, Nusselt number, entropy generation and Bejan number were obtained analytically. The slip effect on flow and thermal fields of Ostwald–de Waele power law fluid in circular microchannel are studied by Barkhordari and Etemad [19] using control volume finite difference method. The slip velocity in their study is defined as a constant coefficient of mean velocity of fluid and thermal boundary conditions are considered constant temperature and constant heat flux at wall. Eventually, the influence of slip coefficient on friction factor and Nusselt number were investigated. Mahjoob et al [20] performed a similar research in rectangular microchannel. To the best of our knowledge, the slip effect on convective heat transfer of viscoelastic fluid, with effect of critical shear stress in slip model, has not been yet investigated. Then, we propose in the present study an analytical approach of forced convection heat transfer in pipe for laminar, steady state and fully developed flow of nonlinear viscoelastic fluid obeying Giesekus model with accounting slip effect. The slip law at wall employed is the nonlinear Navier one with non-zero slip critical shear stress. The canonical geometry of pipe flow is considered in the present paper regarding its wide range of applications.

2. Governing Equation

The problem under consideration is steady, laminar, thermally and hydrodynamically fully developed flow in a pipe (see Fig. 2). Axial heat conduction is neglected compared to the radial heat transfer by the order of magnitude analysis [21]. The effect of viscous dissipation is included due to the high viscosity of viscoelastic fluids considered. Thermophysical properties of fluid are taken independent of temperature. This assumption sounds reasonable since temperature variations are not high enough to significantly change fluid properties [22-24].
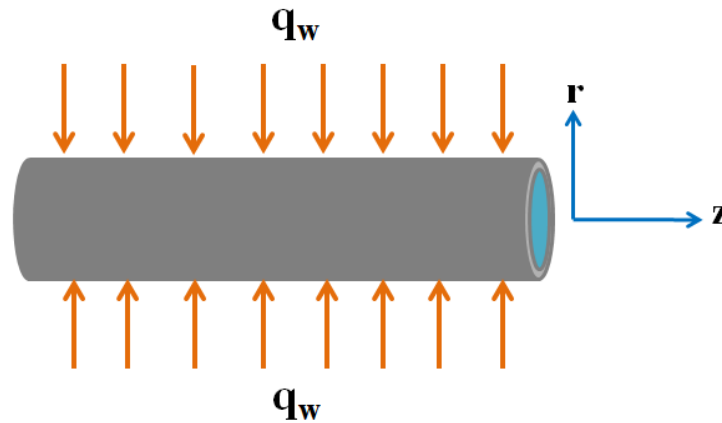
The continuity, momentum and Giesekus constitutive equations (without retardation time) are:

$$\nabla . u = 0 \tag{3-a}$$

$$\rho \frac{Du}{Dt} + \nabla P = \nabla . \tau \tag{3-b}$$

$$\tau + \frac{\alpha \lambda}{\eta}(\tau . \tau) + \lambda \frac{\vartheta \tau}{\vartheta t} = \eta \dot{\gamma} \tag{3-c}$$

Where

$$\dot{\gamma} = [\nabla u + (\nabla u)^T] \tag{4}$$

$$\frac{\vartheta \tau}{\vartheta t} = \frac{D\tau}{Dt} - [\tau . \nabla u + (\nabla u)^T . \tau] \tag{5}$$

$$\frac{D\tau}{Dt} = \frac{\partial \tau}{\partial t} + (u . \nabla) \tau \tag{6}$$

η and λ are the model parameters representing zero shear viscosity and zero shear relaxation time, respectively [25]. In particular, the zero shear relaxation time is corresponding to the time that the stresses arising from shear rate relax after the fluid motion has stopped, which is characteristic of viscoelastic fluids [26]. The model parameters are function of shear rate. They approach to a constant value at very low shear rate which are named zero shear model parameters. Parameter α in Eq.3-c, lying in the range $0 \le \alpha \le 1$ [27] is a mobility factor. The term containing α in the constitutive equation is attributed to anisotropic Brownian motion and/or anisotropic hydrodynamic drag on the constituent polymer molecules [23].

Dimensionless quantities are as follows:

$$r^* = \frac{r}{R} \qquad z^* = \frac{z}{R} \qquad u^* = \frac{u_z}{U} \qquad \gamma^{\circ *} = \frac{\gamma^{\circ}}{U/R} \qquad \tau^* = \frac{\tau}{\eta U/R} \qquad \psi = \frac{R^2}{\eta U}\left(\frac{dp}{dz}\right)$$

Where *U* is the average velocity over cross-section of the pipe and described as follows:

$$U = \frac{\int_0^R 2\pi r u_z \, dr}{\int_0^R 2\pi r \, dr}$$

(7)

3. Analytical solution

3.1 Hydrodynamic solution

The shear stress equation is derived from Eq 3-b as follows:

$$\tau_{rz}^* = \frac{\psi r}{2}$$

(8)

The shear rate equation was derived from Giesekus equation by Yoo and Choi [28] as follows:

$$\gamma_{rz}^* = \frac{du^*}{dr^*} = 2\alpha\tau_{rz}^* \frac{1 \pm (2\alpha - 1)\sqrt{1 - 4\alpha^2 De^2 \tau_{rz}^{*2}}}{\left(2\alpha - 1 \pm \sqrt{1 - 4\alpha^2 De^2 \tau_{rz}^{*2}}\right)^2}$$

(9)

De is the Deborah number, defined as ($De = \lambda U / R$), which is related to the level of fluid elasticity.

The dimensionless form of the slip boundary conditions is as follows:

$$\begin{cases} u_w^* = 0 & \left|\tau_{rzw}^*\right| \leq B_C \\ u_w^* = \left(\frac{\left|\tau_{rzw}^*\right| - B_C}{B}\right)^{\frac{1}{s}} & \left|\tau_{rzw}^*\right| > B_C \end{cases}$$

(10)

B and B_C are dimensionless slip number and dimensionless slip critical shear stress number respectively and are defined as follows:

$$B = \frac{\beta R U^{s-1}}{\eta} \qquad B_c = \frac{\tau_c R}{\eta U}$$

The positive and negative signs of Eq.9 are referred to upper and lower branch solutions, respectively. Yoo and Choi [28] by employing thermodynamic considerations, and Schleiniger and Weinacht [29] using linear stability analysis and considering requirements arising from configuration tensor reached to the same restrictions for the case of no-solvent viscosity of Giesekus model as follows:

6

For the upper branch solution:

$$\left|\tau_{rz}^{*}\right| < \frac{1}{De}\sqrt{\frac{1}{\alpha}-1} \qquad 0 < \alpha \leq \frac{1}{2} \tag{11-a}$$

$$\left|\tau_{rz}^{*}\right| \leq \frac{1}{2\alpha De} \qquad \frac{1}{2} < \alpha \leq 1 \tag{11-b}$$

For the lower branch solution:

$$\frac{1}{De}\sqrt{\frac{1}{\alpha}-1} < \left|\tau_{rz}^{*}\right| \leq \frac{1}{2\alpha De} \qquad \frac{1}{2} < \alpha \leq 1 \tag{12}$$

Since the Giesekus model exhibits unrealistic behavior in range $\frac{1}{2} < \alpha \leq 1$ [23, 28], the lower branch solution is not valid and only the upper branch solution (Eq.11-a) is considered.

In order to reduce the complexity of the problem, an approximate solution approach which has been suggested in references [30-32] is employed. To do so, the term $\sqrt{1-4\alpha^{2}De^{2}\tau_{rz}^{*}{}^{2}}$ in Eq. 9 can be expressed by a power series using the binominal expansion:

$$\sqrt{1-4\alpha^{2}De^{2}\tau_{rz}^{*}{}^{2}} \cong 1-2\alpha^{2}De^{2}\tau_{rz}^{*}{}^{2} \tag{13}$$

where all terms of higher order have been neglected compared to the leading term in the approximation which is valid for small values of $4\alpha^{2}De^{2}\tau_{rz}^{*}{}^{2}$. Truncation error is less than 6% when $4\alpha^{2}De^{2}\tau_{rz}^{*}{}^{2}$ is less than 1/2 (6% relative to the exact value of $\sqrt{1-4\alpha^{2}De^{2}\tau_{rz}^{*}{}^{2}}$). Therefore when $4\alpha^{2}De^{2}\tau_{rz}^{*}{}^{2} < 1/2$ or $\left|\tau_{rz}^{*}\right| < 1/2\sqrt{2}\,\alpha De$, the accuracy of approximation is more than 94%. Noting that in equation ($\left|\tau_{rz}^{*}\right| < 1/2\sqrt{2}\,\alpha De$), τ_{rz}^{*} is function of De and α, it therefore implicitly indicates conditions for having acceptable approximation errors. Hence the relevant constitutive stability condition, i.e. Eq. (11-a) and the approximation validity condition i.e. $\left|\tau_{rz}^{*}\right| < 1/2\sqrt{2}\,\alpha De$ should be simultaneously satisfied [30-32]. It should be noted that including effect of slip condition causes $\left|\tau_{rz}^{*}\right|$ to largely reduce and thus $4\alpha^{2}De^{2}\tau_{rz}^{*}{}^{2}$ is much less than ½ for a wide range of α and De and accuracy of approximation would be higher than 94%. Also slightly away from the wall, $\left|\tau_{rz}^{*}\right|$ decreases which causes $4\alpha^{2}De^{2}\tau_{rz}^{*}{}^{2}$ to decrease

7

and thus accuracy increases again [4]. Approximated and exact solutions are compared in section 4.

By substituting Eq. (13) in Eq. (9) and integrating, dimensionless velocity profile can be obtained as follows:

$$\int_{1}^{r^*} \overset{\circ}{\gamma}_{rz}^* \, dr^* = V^* \Big|_{1}^{r^*} \tag{14}$$

With

$$V^* = \frac{\psi}{A}\left(\frac{8(\alpha-1)}{(Ar^{*2}-4)} + (1-2\alpha)\mathrm{Ln}[Ar^{*2}-4]\right)$$

and $A = De^2\alpha\psi^2$

Then we obtained

$$u^* = V^* \Big|_{1}^{r^*} + u_w^*$$

With

$$u_w^* = \left(-\frac{\psi + 2B_c}{2B}\right)^{\frac{1}{s}}$$

ψ is an unknown parameter in the velocity profile. To determine it, a dimensionless average velocity definition is employed. It can be noted that u_w^* depends on the critical shear stress via the term B_c.

Dimensionless form of Eq. 7 is as below:

$$\int_{0}^{1} r^* u^* \, dr^* = \frac{1}{2} \tag{15}$$

By integrating in Eq.15, the equation for determining ψ is obtained as follows:

$$\frac{12\psi + \alpha\psi\left(U_1 + U_2 - 16\right)}{2A(A-4)} + \frac{U_3}{A^2} = \frac{1}{2} \tag{16}$$

with

$$U_1 = De^2 \psi^2 (2\alpha - 1) \qquad U_2 = De^2 \psi \left(-\frac{B_C}{B} - \frac{\psi}{2B} \right)^{\frac{1}{s}} (A-4) \qquad U_3 = 2\psi(4\alpha - 3)\operatorname{Ln}[(4-A)/4]$$

ψ is determined by solving Eq. 16.

3.2 Thermal solution

Hydrodynamic solution has been determined in section 3.1. Since thermophysical parameters are assumed to be independent of the temperature, the hydrodynamic solution is decoupled from the energy equation. This allows us to determine the temperature profiles analytically. The energy equation with considering assumptions can be represented by the following equation:

$$\rho c_p u_z \frac{\partial T}{\partial z} = \frac{k}{r} \frac{\partial}{\partial r} \left(r \frac{\partial T}{\partial r} \right) + \Phi \tag{17}$$

Where c_p, ρ and k are specific heat capacity , density and thermal conductivity of the fluid, respectively. T is temperature and Φ is dissipation function which includes only the shear stress and shear rate for this flow.

$$\Phi = \tau_{rz} \frac{\partial u_z}{\partial r} \tag{18}$$

The thermal boundary conditions are peripherally and axially constant heat flux at wall and symmetry at the axis.

$$r = R \qquad\qquad k \frac{\partial T}{\partial r} = q_w \tag{19-a}$$

$$r = 0 \qquad\qquad \frac{\partial T}{\partial r} = 0 \tag{19-b}$$

For fully developed temperature profile, the following relation holds [33]:

$$\frac{\partial}{\partial z} \left(\frac{T_w - T}{T_w - T_b} \right) = 0 \tag{20}$$

Where T_w and T_b represent wall and bulk temperatures, respectively. Bulk temperature is defined as follows:

$$T_b = \frac{\int_0^R 2\pi \, ruTdr}{\int_0^R 2\pi \, rudr} \qquad (21)$$

For the imposed heat flux case, Eq.20 reduces to:

$$\frac{\partial T}{\partial z} = \frac{\partial T_w}{\partial z} = \frac{\partial T_b}{\partial z} \qquad (22)$$

Applying energy balance over an infinitesimal element of fluid, dz, the following equation is obtained for axial gradient of fluid bulk temperature.

$$\frac{\partial T_b}{\partial z} = \frac{2}{\rho U c_p R}\left[q_w + \int_0^R r\tau_{zr} \frac{\partial u_z}{\partial r} dr \right] \qquad (23)$$

Eq.24 is obtained by combining Eqs. (17), (22) and (23) and using dimensionless terms.

$$\frac{1}{r^*}\frac{\partial}{\partial r^*}\left(r^* \frac{\partial \Theta}{\partial r^*} \right) = Xu^* - Br\Phi^* \qquad (24)$$

Where

$$X = 1 + 2Br \int_0^1 r^* \tau^* \frac{\partial u^*}{\partial r^*} dr^* \qquad (25\text{-}a)$$

$$\Phi^* = \tau^* \frac{\partial u^*}{\partial r^*} \qquad (25\text{-}b)$$

Detail regarding X is presented in the Appendix A.

Θ is the dimensionless local temperature and Br is the dimensionless Brinkman number, which is a measure of importance of the viscous dissipation term.

$$\Theta = \frac{k(T - T_b)}{2Rq_w} \qquad (26) \qquad\qquad Br = \frac{\eta U^2}{2Rq_w} \qquad (27)$$

The dimensionless thermal boundary conditions are as follows:

$$\frac{\partial \Theta}{\partial r^*} = \frac{1}{2} \qquad\qquad r^* = 1 \qquad\qquad (28\text{-}a)$$

$$\frac{\partial \Theta}{\partial r^*} = 0 \qquad\qquad r^* = 0 \qquad\qquad (28\text{-}b)$$

Dimensionless temperature profile (Θ) is obtained by integrating Eq. 24.

$$\Theta = X\overline{U} - Br\overline{\Phi} + C_1 \mathrm{Ln}(r^*) + C_2 \qquad\qquad (29)$$

$$\overline{U} = \int \frac{1}{r^*} \int u^* r^* dr^* dr^* \qquad\qquad (30\text{-}a)$$

$$\overline{\Phi} = \int \frac{1}{r^*} \int \Phi^* r^* dr^* dr^* \qquad\qquad (30\text{-}b)$$

Expressions of $\overline{U}$ and $\overline{\Phi}$ are presented in Appendix A.

Since both boundary conditions are of second type, determination of C_2 value is not possible directly. Hence, C_2 is eliminated from Eq.29 by subtracting the dimensionless wall temperature (Θ_w) from the dimensionless temperature profile (Θ) as shown below.

$$\Theta - \Theta_w = X \left(\overline{U} - \overline{U}\big|_{r^*=1}\right) - Br\left(\overline{\Phi} - \overline{\Phi}\big|_{r^*=1}\right) + C_1 \mathrm{Ln}(r^*) \qquad\qquad (31)$$

C_1 can be obtained as follows:

$$C_1 = \left[Br \frac{d\overline{\Phi}}{dr^*}\bigg|_{r^*=1} - X \frac{d\overline{U}}{dr^*}\bigg|_{r^*=1} - \frac{1}{2} \right] \qquad\qquad (32)$$

By substituting temperature (T) from Eq. 26 into Eq. 21, the following expression for the dimensionless wall temperature is obtained after simplifications:

$$\Theta_w = 2\int_0^1 r^* u^* \left(\Theta_w - \Theta\right) dr^* \qquad\qquad (33)$$

Details of mathematical process for deriving Eq.33 are in Appendix B.

After numerical integration of Eq.(33), we have access to the convective heat transfer between wall and fluid which is quantified by Nusselt number (Nu), defined as ($Nu = 2Rh/k$).The heat transfer coefficient

(h) is obtained from ($q_w = h(T_w - T_b)$). By using dimensionless temperature definition (Eq.26), the Nusselt number at wall becomes:

$$Nu_w = 1/\Theta_w \tag{34}$$

4. Results and Discussion

For the evaluation of our approximation accuracy, the numerical solving for hydrodynamic and energy differential equations is performed without considering the approximate assumption (Eq.13) by MATHEMATICA. A comparison between the exact numerical and approximate analytical solutions is made for the velocity and temperature profiles that are shown in Figs.3-a and 3-b. As it is seen, there is high compliance between results of two solutions. To go further in the thermal part, we have to use the approximated analytical method.
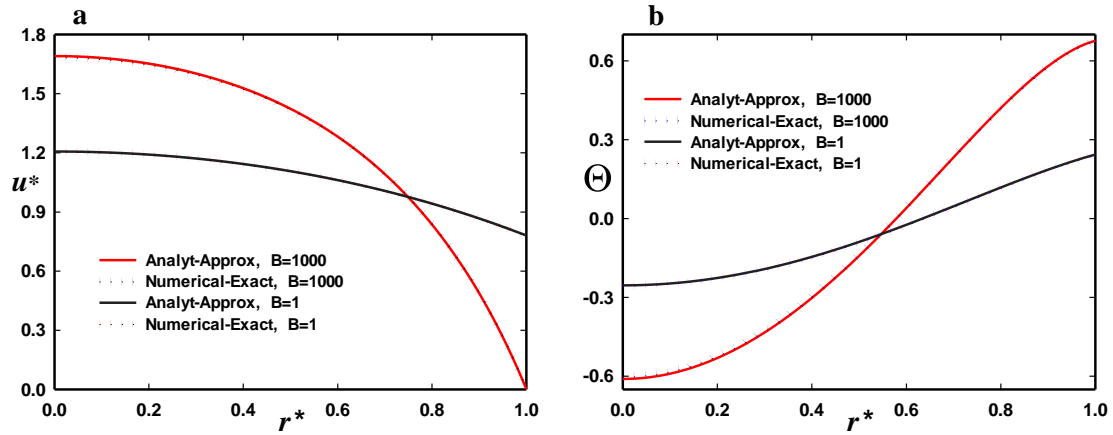
Fig.3- Dimensionless a- velocity profile for α=0.1, De = 1, s = 1 and Bc = 0   b- temperature profile for α=0.1, De = 1, s = 0.5 and Bc = 0.5.

4.1 Wall heating

Fig. 4 shows effect of slip number on velocity profile. It is seen that figure tends to no slip and full slip conditions for B =10000 and B = 0.001 respectively. For full slip case, u_w = 1 and plug flow is recovered. In case of heat transfer it should be noted the viscoelastic fluid behavior during heating ($q_w > 0$) and

12

cooling ($q_w < 0$) processes is different. Figs. 5a-c show effects of Brinkman number and dimensionless slip parameters on Nusselt number for the case of wall heating. From Figs. 5a-c we can notice that the Nusselt number decreases when increasing the Brinkman number because the heat generation by viscous dissipation increases in this case. Since both shear stress and velocity gradient reach their maximum values adjacent to the walls and according to the viscous dissipation function (Eq. 18), the heat generation is stronger near the wall. Therefore, the difference between the wall temperature and the bulk temperature increases and according to the Nusselt number and dimensionless temperature expressions (Eqs. 34 and 26) the Nusselt number decreases.
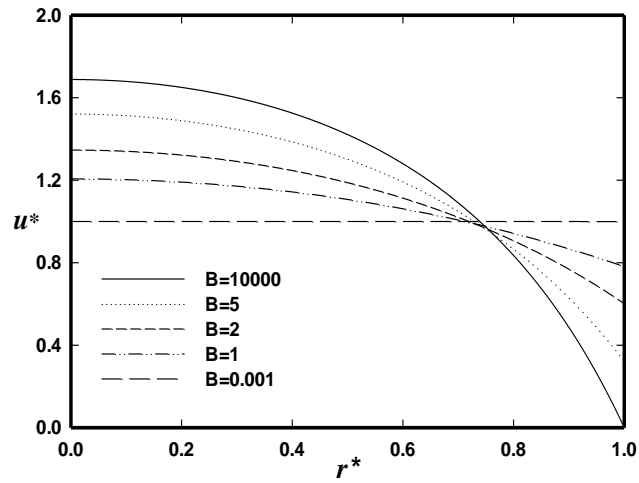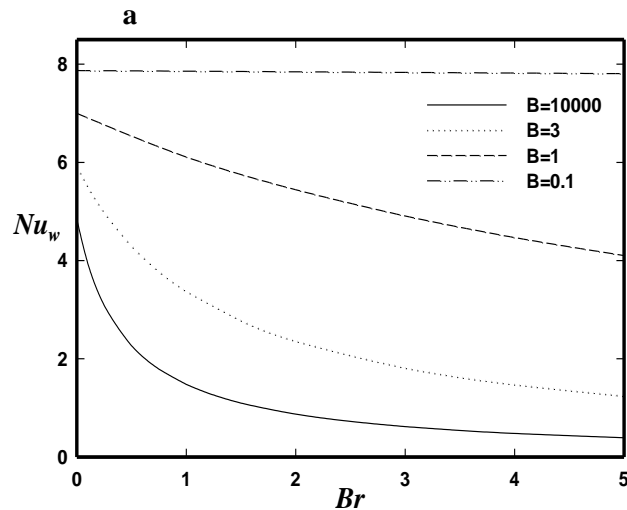

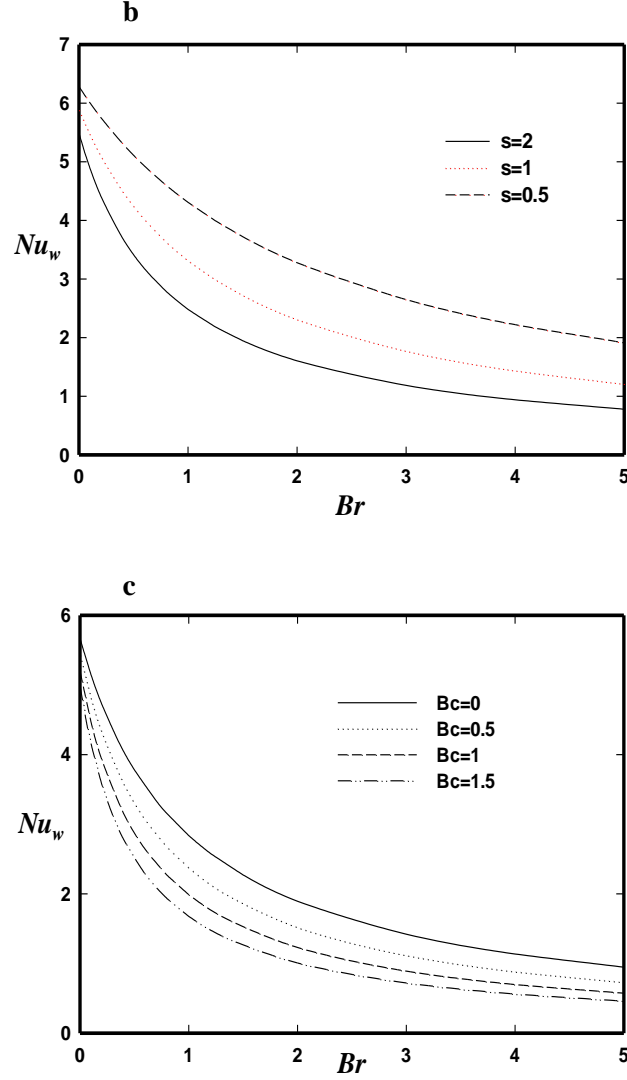Fig.4. Dimensionless velocity profile with variation of the B for α=0.1, De = 1, s = 1 and Bc = 0.

Fig.5. Variation of Nu_w versus Br in the case of fluid heating (Br>0) for $\alpha=0.1$, $De=1$ and a- dimensionless slip number (B) at s=1 and Bc=0 b- power law index of slip (s) at B=2 and Bc=0.5 c- dimensionless slip critical shear stress number (Bc) at B=4 and s=1.

The slip effect on Nusselt number is significant. According to Eq.10, the slip velocity increases by decreasing slip number (B) and slip critical shear stress number (Bc) or increasing power law index of slip (s). Nusselt number increases by increasing slip effect because the slip effect decreases both shear stress and velocity gradient and therefore viscous dissipation is reduced. Decreasing viscous dissipation increases Nusselt number for the reason previously explained. For the full slip case, Nusselt number is independent of Brinkman number because both shear stress and velocity gradient tend to zero and as a

14

result viscous dissipation will be negligible. Figure 6 shows influences of slip parameters on dimensionless temperature distribution. Since the heat generation by viscous dissipation is reduced when slip is increased and since the effect of viscous dissipation is prominent at wall therefore the difference between the wall temperature and the fluid temperature decreases by increasing slip effect.
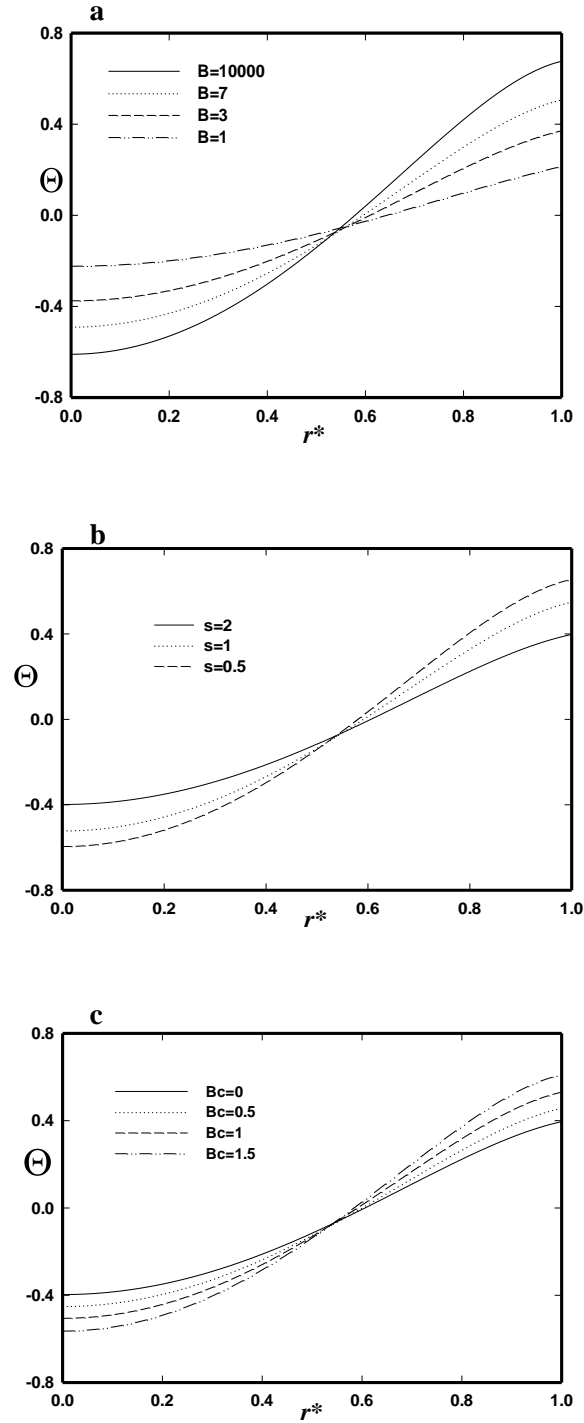
Fig.6. Dimensionless temperature profile with variation of a- dimensionless slip number (B) at s=1 and Bc=0.5   b- power law index of slip (s) at B=6 and Bc=1   c- dimensionless slip critical shear stress number (Bc) at B=5 and s=1 in the case of in the case of fluid heating (Br>0) for α=0.1, De=1 and Br=1.

4.2 Wall cooling

Wall cooling ($q_w < 0$) is applied to reduce the bulk temperature of fluid which is necessary in many industries. In these processes when viscous dissipation is low (small Brinkman number) the fluid temperature along the pipe decreases ($\partial T/\partial z < 0$). By increasing Brinkman number the internal heat generation grows until a critical value for whom this generated heat overcomes the effect of wall cooling and fluid starts to warm up itself. This aforesaid critical Brinkman is called the first critical Brinkman number (Br$_1$), and is determined by equating the dimensionless form of the bulk temperature gradient equation (Eq.25-a) to zero.

$$Br_1 = \frac{-1}{2\int_0^1 r^* \tau^* \frac{\partial u^*}{\partial r^*} dr^*}$$

(35)

Detail regarding Br$_1$ is presented in the Appendix A.

From Fig. 7 we remark that by increasing slip effect (decreasing B and Bc or increasing s), Br$_1$ increases, corresponding to the extension of the fluid cooling range. Since the increasing slip effect reduces inside heat generation by viscous dissipation thus the cooling process can be occurred in the broader range of q$_w$. Another investigations about elasticity effect on critical Brinkman number [24, 34] show that reduction of viscous dissipation by increasing elasticity has a similar influence with increasing slip effect on this critical Brinkman number (Br$_1$) .
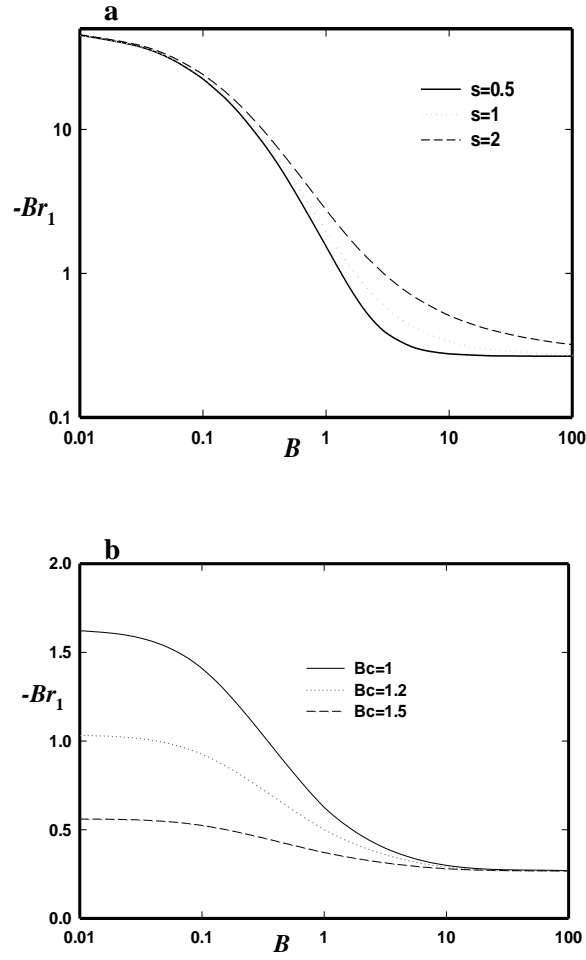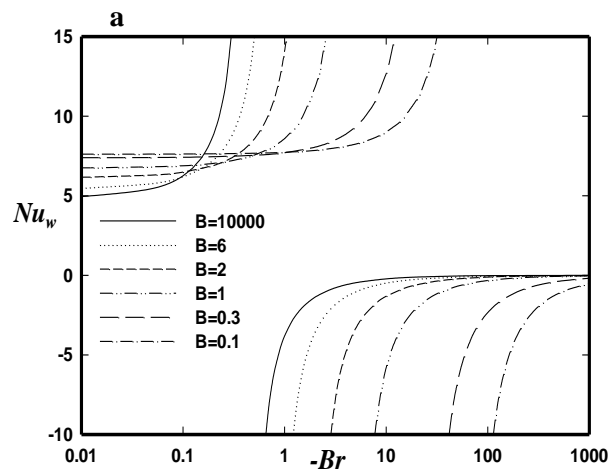
16

Fig.7. Variation of first critical Brinkman number (Br_1) versus dimensionless slip number (B) in the case of fluid cooling (Br<0) for $\alpha=0.1$, De=1 and a- power law index of slip (s) at Bc=0.2   b- dimensionless slip critical shear stress number (Bc) at s=1.

Effects of Brinkman number and slip parameters on Nusselt number are shown in Fig.8 for the case of wall cooling. It is seen that Nusselt number is positive at low Brinkman numbers and shows a singularity in a Brinkman number larger than the first critical Brinkman which is called second critical Brinkman number (Br_2). Eventually Nusselt number can be negative at high Brinkman numbers. In the case of wall cooling because of negative heat flux in the wall, the wall temperature is lower than the bulk temperature and since the flux sign is also negative according to the dimensionless temperature and Nusselt number expressions (Eqs. 26 and 34), Nusselt becomes positive. The growth of Brinkman number increases the heat generated by viscous dissipation. Since the heat generation is stronger near the wall, the difference between the bulk temperature and the wall temperature decreases and

17

subsequently Nusselt number increases. At the second critical Brinkman number the wall temperature will be equal to the bulk temperature and as a result Nusselt number approaches infinity. For $|Br|>|Br_2|$, the wall temperature becomes higher than the bulk temperature and thus Nusselt becomes negative. Also if the Brinkman number increases even more, the difference between the wall temperature and the bulk temperature increases and Nusselt number approaches to zero. The second critical Brinkman number increases by increasing slip effect (increasing s or decreasing B and Bc) which means that the singularity in Nusselt curve occurs at higher Brinkman number. Because increasing slip effect decreases heat generated by viscous dissipation therefore, reduction of the difference between the bulk temperature and the wall temperature will be occur at higher Brinkman number. Also, increasing slip effect increases Nusselt number at negligible Brinkman number because slip effect causes to fluid flow rate increase adjacent to the wall and therefore, resistance to heat transfer between wall and fluid decreases. In this case viscous dissipation does not have a role in the variation of the Nusselt number. Viscous dissipation effect will be important at larger Brinkman number but leading to opposite behaviors when $|Br|<|Br_2|$ and $|Br|>|Br_2|$. For $|Br|<|Br_2|$, the wall temperature is lower than the bulk temperature. Since the slip effect reduces the heat generation by viscous dissipation therefore the difference between the bulk temperature and the wall temperature increases and consequently Nusselt number decreases. Reversely, when $|Br|>|Br_2|$ the wall temperature is higher than the bulk temperature and by increasing slip effect the difference between the wall temperature and the bulk temperature decreases and hence, Nusselt number increases.
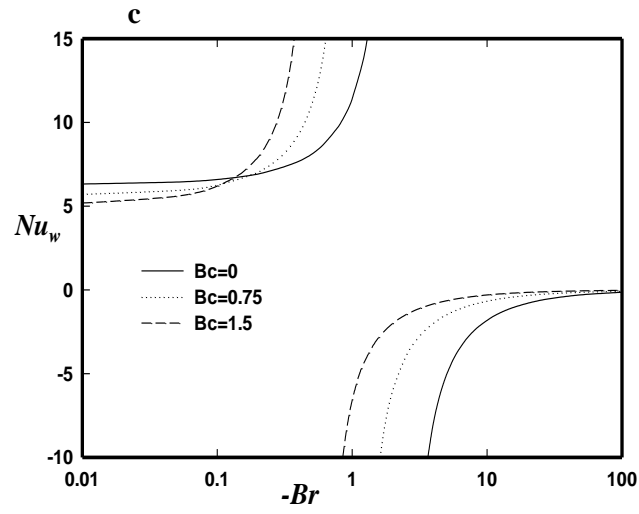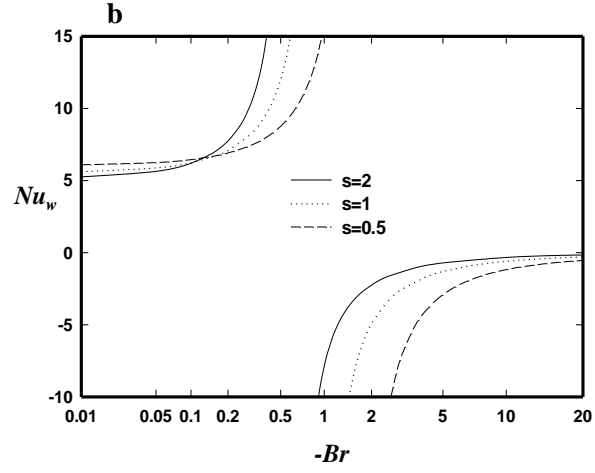
Fig.8. Variation of Nu_w versus Br in the case of fluid cooling (Br<0) for α=0.1, De=1 and a- dimensionless slip number (B) at s=1 and Bc=0.2 b- power law index of slip (s) at B=3 and Bc=0.5 c- dimensionless slip critical shear stress number (Bc) at B=2 and s=1.
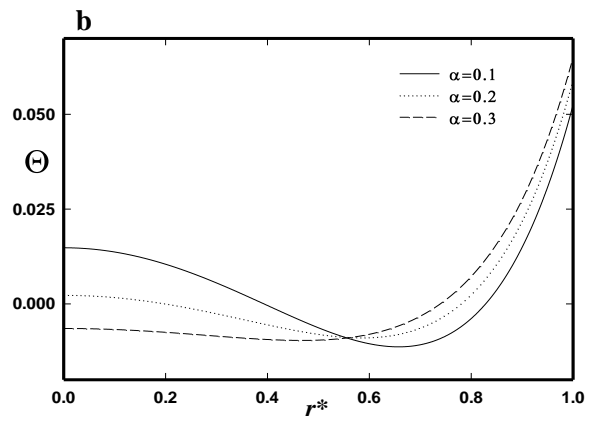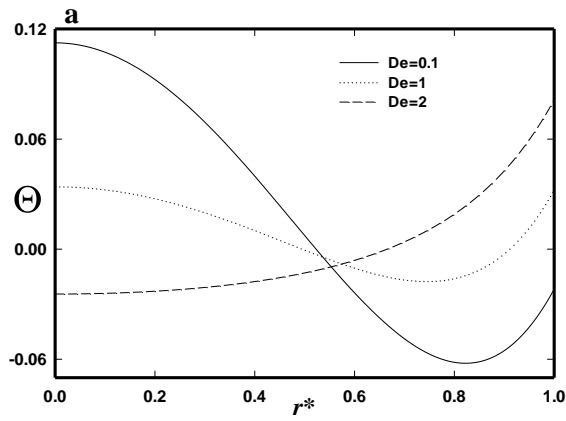

19

Fig.9 shows the effect of fluid elasticity (Deborah number and mobility factor) on dimensionless temperature distribution for fluid cooling case. As can be seen from the trend of temperature profile changes by increasing elasticity because the first critical Brinkman number (Br_1) increases with the elasticity. This means that for higher values of elasticity (De=2 in Fig.9-a and $\alpha = 0.3$ in Fig.9-b), |Br| is smaller than |Br_1| and the fluid is cooling. For lower values of elasticity, |Br| is larger than |Br_1| and the fluid is heating. For the cooling case the minimum temperature is at the wall. This is not the case for the heating case where the effect of viscous dissipation is strengthened due to decreasing elasticity. Since the effect of viscous dissipation is prominent at wall therefore the internal heat generated increases the wall temperature so that at small value of elasticity (De=0.1) the wall temperature will be higher than the bulk temperature.

5. Conclusions

Analytical solutions for hydrodynamics and convective heat transfer of viscoelastic fluid obeying Giesekus model was obtained in pipes under steady, laminar, thermal and hydrodynamical fully developed conditions. The nonlinear Navier slip law was employed at wall when the wall shear stress reaches a critical value which is known as slip critical shear stress. Thermal boundary condition was peripherally and axially constant heat flux at wall. Analysis was performed for both cases of fluid heating (Br > 0) and fluid cooling (Br < 0). Effects of slip parameters (B, Bc and s), viscous dissipation (Br) and fluid elasticity (De and α) were investigated on Nusselt number and dimensionless temperature profile. For the heating case, the Nusselt number increases when increasing the slip effect and decreases by increasing the Brinkman number. For the cooling case, when |Br|>|Br_1| the heat generated internally by viscous dissipation overcomes the effect of wall cooling and fluid starts to warm up. Also the Nusselt curve showed a singularity in a second critical Brinkman number (Br_2) and then change of sign. Slip effect reduces viscous dissipation, thus increasing the cooling range.

Appendix A

$$X = 1 + 2Br\psi^2 \left(\left(\frac{4(\alpha-1)AR^2}{A^2(AR^2-4)} - \frac{(2\alpha-1)AR^2}{2A^2} - \frac{(8\alpha-6)\text{Ln}[(4-AR^2)/4]}{A^2} \right) \right)$$

$$\overline{U} = \frac{\psi}{2A^2} \left(\frac{1}{2}(2\alpha-1)\left(Ar^2(\text{Ln}[Ar^2-4]-2) - 4\text{Ln}[4-Ar^2] \right) - 4\text{Ln}[r]\left(2\alpha-1+(4\alpha-3)\text{Ln}[\frac{4-Ar^2}{4Ar^2-16}] \right) + (6-8\alpha)\text{Li}_2\left(\frac{Ar^2}{4} \right) \right)$$

$$+ \frac{r^2}{4}\left(\left(-\frac{B_C}{B} - \frac{\psi}{2B} \right)^{\frac{1}{S}} - \frac{\psi}{A}\left(\frac{8(\alpha-1)}{A-4} \right) + (1-2\alpha)\text{Ln}[A-4] \right)$$

$$\overline{\Phi} = -\frac{\psi^2}{2A^2}\left(\frac{Ar^2}{2}(2\alpha-1) - 4(\text{Ln}[r]+(\alpha-1)\text{Ln}[4-Ar^2]) - 2(4\alpha-3)\left(2\text{Ln}[r]\text{Ln}[\frac{4-Ar^2}{4Ar^2-16}] + \text{Li}_2\left(\frac{Ar^2}{4} \right) \right) \right)$$

$$Br_1 = \frac{Br}{1-X} \qquad \text{Li}_n(z) = \sum_{k=1}^{\infty} \frac{z^k}{k^n}$$

Appendix B

$$T_b = \frac{\int_0^R 2\pi\, ruTdr}{\int_0^R 2\pi\, rudr} = \frac{\int_0^1 r^*u^*Tdr^*}{\int_0^1 r^*u^*dr^*} \qquad\qquad\qquad\qquad \text{(B-1)}$$

By using Eq.15, the bulk temperature becomes:

$$T_b = 2\int_0^1 r^*u^*Tdr^* \qquad\qquad\qquad\qquad \text{(B-2)}$$

By substituting temperature (T) from Eq. 26 into Eq. B-2, the following expressions for the bulk temperature is obtained:

$$T_b = 2\int_0^1 r^*u^*\left(\frac{2q_wR}{k}\Theta + T_b \right)dr^* = \frac{4q_wR}{k}\int_0^1 r^*u^*\Theta dr^* + 2T_b\underline{\int_0^1 r^*u^*dr^*} \qquad \text{(B-3)}$$

Using Eq.15, we can write:

$$T_b = \frac{4q_wR}{k}\int_0^1 r^*u^*\Theta dr^* + T_b \qquad\qquad\qquad\qquad \text{(B-4)}$$

Consequently

$$\int_0^1 r^* u^* \Theta \, dr^* = 0 \tag{B-5}$$

Since the wall temperature is not radial function ($\Theta_w = f(R) \neq f(r)$), we can write as follows:

$$\Theta_w = 2\Theta_w \int_0^1 r^* u^* dr^* = 2\int_0^1 r^* u^* \Theta_w dr^* \tag{B-6}$$

Finally Eq.B-7 is obtained by subtraction of Eq. B-6 from B-5.

$$\Theta_w = 2\int_0^1 r^* u^* (\Theta_w - \Theta) dr^* \tag{B-7}$$

References

[1] R.P.Chhabra, J. F. Richardson , Non-Newtonian flow in the process industries: Fundamentals and engineering applications, Oxford: Butterworth-Heinemann,1999

[2] H.Yamaguchi, Engineering fluid mechanics. Springer-Verlag, Dordrecht, 2008

[3] M.M. Denn, Extrusion instabilities and wall slip, Annu. Rev. Fluid Mech. 33 (2001) 265–287.

[4] M.M. Mohseni, F. Rashidi, Axial annular flow of a Giesekus fluid with wall slip above the critical shear stress, J. Non-Newton. Fluid Mech. 223 (2015) 20–27.

 [5] Y. Damianou, M. Philippou, G. Kaoullas, G.C. Georgiou, Cessation of viscoplastic Poiseuille flow with wall slip, J. Non-Newton. Fluid Mech. 203 (2014) 24–37.

[6] L.L. Ferras, J.M. Nobrega, F.T. Pinho, Analytical solutions for Newtonian and Inelastic non-Newtonian flows with wall slip, J. Non-Newton. Fluid Mech. 175– 176 (2012) 76–88.

[7] L.L. Ferras, J.M. Nobrega, F.T. Pinho, Analytical solutions for channel flows of Phan–Thien–Tanner and Giesekus fluids under slip, J. Non-Newton. Fluid Mech. 171–172 (2012) 97–105.

[8] M.T. Matthews, J.M. Hill, Newtonian flow with nonlinear Navier boundary condition, Acta Mech. 191 (2007) 195–217.

[9] M. Chatzimina, G.C. Georgiou, K. Housiadas, S.G. Hatzikiriakos, Stability of the annular Poiseuille flow of a Newtonian liquid with slip along the walls, J. NonNewton. Fluid Mech. 159 (2009) 1–9.

[10] D.M. Kalyon, M. Malik, Axial laminar flow of viscoplastic fluids in a concentric annulus subject to wall slip, Rheol. Acta 51 (2012) 805–820.

[11] G.G. Pereira, Effect of variable slip boundary conditions on flows of pressure driven non-Newtonian fluids, J. Non-Newton. Fluid Mech. 157 (2009) 197–206.

[12] G. Kaoullas, G.C. Georgiou, Newtonian Poiseuille flows with wall slip and nonzero slip yield stress, J. Non-Newton. Fluid Mech. 197 (2013) 24–30.

[13] K.D. Housiadas, Viscoelastic Poiseuille flows with total normal stress dependent, nonlinear Navier slip at the wall, Phys. Fluids 25 (2013). 043105-1-21.

[14] Y. Damianou, G.C. Georgiou, I. Moulitsas, Combined effects of compressibility and slip in flows of a Herschel–Bulkley fluid, J. Non-Newton. Fluid Mech. 193 (2013) 89–102.

[15] H.S. Tang, D.M. Kalyon, Unsteady circular tube flow of compressible polymeric liquids subject to pressure-dependent wall slip, J. Rheol. 52 (2) (2008) 507–526.

[16] H.S. Tang, D.M. Kalyon, Time-dependent tube flow of compressible suspensions subject to pressure dependent wall slip: ramifications on development of flow instabilities, J. Rheol. 52 (5) (2008) 1069–1090.

[17] V.Anand, Slip law effects on heat transfer and entropy generation of pressure driven flow of a power law fluid in a microchannel under uniform heat flux boundary condition, Energy 76 (2014) 716-732.

[18] M.Shojaeian, A.Kosar, Convective heat transfer and entropy generation analysis on Newtonian and non-Newtonian fluid flows between parallel-plates under slip boundary conditions, International Journal of Heat and Mass Transfer 70 (2014) 664–673.

[19] M. Barkhordari, S.Gh. Etemad, Numerical study of slip flow heat transfer of non-Newtonian fluids in circular microchannels, International Journal of Heat and Fluid Flow 28 (2007) 1027–1033.

[20] M. R. Mahjoob, S.Gh. Etemad,J. Thibault, Numerical Study of Non-Newtonian Flow Through Rectangular Microchannels, Iranian Journal of Chemical Engineering, 6 (2009) 44–61.

[21] S. Kakac, Y.Yener , Convective Heat Transfer, CRC Press (1995).

[22] P.J. Oliveira, F.T. Pinho, Analysis of forced convection in pipes and channels with the simplified Phan-Thien–Tanner fluid, Int. J. Heat Mass Transfer 43 (13) (2000) 2273–2287.

[23] R.B. Bird, R.C. Armstrong, O. Hassager, Dynamics of polymeric liquids, second ed., vol. 1, Wiley, New York, 1987.

[24] M.M. Mohseni, F. Rashidi, M. R. Khorsand Movagar, Analysis of Forced Convection Heat Transfer for Axial Annular Flow of Giesekus Viscoelastic Fluid, Korean Chem. Eng. Res. 53 (2015) 91-102.

[25] H. Giesekus, Stressing behavior in simple shear flow as predicted by a new consecutive model for polymer fluids, J. Non-Newton. Fluid Mech. 12 (1983) 367–374.

[26] R.B. Bird, W.E. Stewart, E.N Lightfoot, Transport Phenomena, second ed., Wiley, New York, 2001.

[27] H. Giesekus, A simple constitutive equation for polymer fluids based on the concept of deformation-dependent tensorial mobility, J. Non-Newton. Fluid Mech. 11 (1982) 69–109.

[28] J.Y. Yoo, H.Ch. Choi, On the steady simple shear flows of the one-mode Giesekus fluid, Rheol. Acta 28 (1989) 13–24.

[29] G. Schleiniger, R. Weinacht, Steady Poiseuille flows for a Giesekus fluid, J. NonNewton. Fluid Mech. 40 (1991) 79–102.

[30] M. Jouyandeh, M. Moayed Mohseni, F. Rashidi, Tangential Flow Analysis of Giesekus Model in Concentric Annulus with Both Cylinders Rotation, J.Applied Fluid Mechanics 10 (2017) 1721–1728.

[31] A. Raisi, M. Mirzazadeh, A. Dehnavi, F. Rashidi, An approximate solution for the Couette–Poiseuille flow of the Giesekus model between parallel plates, Rheol. Acta 47 (2008) 75–80.

[32] M.M. Mohseni, F. Rashidi, Viscoelastic fluid behaviour in annulus using Giesekus model, J. Non-Newton. Fluid Mech. 165 (2010) 1550–1553.

[33] A. Bejan, Convection heat transfer. Wiley, New York, 1995.

[34] A.Mahdavi Khatibi, M. Mirzazadeh, F. Rashidi, Forced convection heat transfer of Giesekus viscoelastic fluid in pipes and channels, Heat Mass Transfer 46 (2010) 405–412.